# Role of the $N^*(1535)$ in the $\Lambda_c^+ \to \bar{K}^0 \eta p$ decay

Ju-Jun Xie[1] and Li-Sheng Geng[2,*]

[1]*Institute of Modern Physics, Chinese Academy of Sciences, Lanzhou 730000, China*
[2]*School of Physics and Nuclear Energy Engineering and International Research Center
for Nuclei and Particles in the Cosmos and Beijing Key Laboratory of Advanced
Nuclear Materials and Physics, Beihang University, Beijing 100191, China*

The nonleptonic weak decay of $\Lambda_c^+ \to \bar{K}^0 \eta p$ is analyzed from the viewpoint of probing the $N^*(1535)$ resonance, which has a big decay branching ratio to $\eta N$. Up to an arbitrary normalization, the invariant mass distribution of $\eta p$ is calculated with both the chiral unitary approach and an effective Lagrangian model. Within the chiral unitary approach, the $N^*(1535)$ resonance is dynamically generated from the final-state interaction of mesons and baryons in the strangeness zero sector. For the effective Lagrangian model, we take a Breit-Wigner formula to describe the distribution of the $N^*(1535)$ resonance. It is found that the behavior of the $N^*(1535)$ resonance in the $\Lambda_c^+ \to \bar{K}^0 N^*(1535) \to \bar{K}^0 \eta p$ decay within the two approaches is different. The proposed $\Lambda_c^+$ decay mechanism can provide valuable information on the properties of the $N^*(1535)$ and can in principle be tested by facilities such as BEPC II and SuperKEKB.

## I. INTRODUCTION

Understanding the nature of the $N^*(1535)$ with spin parity $J^P = 1/2^-$ has always been one of the most challenging topics in hadron physics [1,2]. In classical constituent quark models, the $N^*(1535)$ is mainly composed of three valence quarks, and its mass should be lower than the radial excitation, the $N^*(1440)$, with $J^P = 1/2^+$ [3,4]. This is the long-standing mass reverse problem for the lowest spatial excited nucleon states. Another peculiar property of the $N^*(1535)$ is that it couples strongly to the channels with strangeness, such as $\eta N$ and $K\Lambda$, which is also difficult to understand in the naive constituent quark models.

Renouncing the picture of baryons as three-quark bound states, a different point of view consists in describing meson-baryon scattering reactions by taking mesons and baryons as the relevant degrees of freedom at low energies. Then, baryon excited states manifest themselves as poles of the meson-baryon scattering amplitude in a certain Riemann sheet in the complex energy plane. For example, the unitary extensions of chiral perturbation theory have brought new light to studies of baryon resonances from meson-baryon interactions [5,6]. In the chiral unitary coupled-channel approach it was found that the $N^*(1535)$ resonance is dynamically generated as a meson-baryon state with its mass, width, and branching ratios in fair agreement with experiments [7–13]. The numerical results obtained in those studies differ to some extent, but it was found that the $N^*(1535)$ resonance couples strongly to the $\eta N$ channel. Furthermore, it couples more strongly to $K\Sigma$ and $K\Lambda$ than to $\pi N$ [8–13].

In the phenomenological studies, besides the large coupling of the $N^*(1535)$ to $\eta N$, a large value of the coupling of the $N^*(1535)$ to $K\Lambda$ is deduced in Refs. [14–16] by a simultaneous fit to the BES data on $J/\psi \to p\bar{p}\eta$, $pK^-\bar{\Lambda} + \bar{p}K^+\Lambda$; the COSY data on $pp \to pK^+\Lambda$; and the CLAS data on the $\gamma p \to K^+\Lambda$ reaction. There is also evidence for a large coupling of the $N^*(1535)$ to $\eta'N$ from the analysis of the $\gamma p \to p\eta'$ reaction [17] and $pp \to pp\eta'$ reaction [18], and a large coupling of the $N^*(1535)$ to $\phi N$ from the $\pi^- p \to n\phi$, $pp \to pp\phi$, and $pn \to d\phi$ reactions [19–21].

The above-mentioned strange decay properties of the $N^*(1535)$ resonance can be easily understood if it contains large five-quark components [14,22,23]. Within the penta-quark picture, the $N^*(1535)$ resonance could be the lowest $L = 1$ orbital excited $uud$ state with a large admixture of $[ud][us]\bar{s}$ pentaquark components having $[ud]$, $[us]$, and $\bar{s}$ in the ground state. This makes the $N^*(1535)$ heavier than the $N^*(1440)$ and also gives a natural explanation of its larger couplings to the channels with strangeness [24–26].

One should note that the properties of the $N^*(1535)$ were derived from the partial wave analysis of pion- and photon-induced reactions off the nucleon [27–38], where the pole position $(M_{\text{pole}} - i\Gamma_{\text{pole}}/2)$ can be identified from the zero of the denominator of the fitted scattering amplitude in the complex plane. Because the $N^*(1535)$ couples very strongly to the $\eta N$ channel, and the $\eta N$ mass threshold is close to the mass of the $N^*(1535)$, the obtained $N^*(1535)$ Breit-Wigner (BW) parameters, $M_{\text{BW}}$ and $\Gamma_{\text{BW}}$, deviate from its pole parameters by a large amount and are reaction dependent [4]. Indeed, Ref. [27] gives $M_{\text{BW}} = 1547$ MeV and $\Gamma_{\text{BW}} = 188$ MeV, while the obtained pole position is at $1502 - i95/2$ MeV. However, all the latest partial wave

*lisheng.geng@buaa.edu.cn

analyses [33–38] give a rather stable pole position with mass around 1500 MeV and width around 110 MeV.

Recently, it has been shown that the nonleptonic weak decays of charmed hadrons provide a useful platform to study hadronic resonances, some of which are subjects of intense debate about their nature [39,40]. For instance, the $\Lambda_c^+ \to \pi^+ MB$ weak decays are studied in Ref. [41] from the viewpoint of probing the $\Lambda(1405)$ and $\Lambda(1670)$ resonances, where $M$ and $B$ stand for mesons and baryons. In Ref. [42], the $\pi\Sigma$ mass distribution was studied in the $\Lambda_c^+ \to \pi^+\pi\Sigma$ decays with the aim of extracting the $\pi\Sigma$ scattering lengths. In Ref. [43], the $a_0(980)$ and $\Lambda(1670)$ states were investigated in the $\Lambda_c^+ \to \pi^+\eta\Lambda$ decay, taking into account the $\pi^+\eta$ and $\eta\Lambda$ final-state interactions. The pure $I = 1$ nature of the $\pi^+\eta$ channel is particularly beneficial to the study of the $a_0(980)$ state. The role of the $\Sigma^*(1380)$ state with $J^P = 1/2^-$ in the $\Lambda_c^+ \to \eta\pi^+\Lambda$ decay is also studied in Ref. [44], where the color-suppressed $W$-exchange diagram is considered for the production of the $\Sigma^*(1385)$ with $J^P = 3/2^+$. In Ref. [45] the role of the exclusive $\Lambda_c^+$ decays into a neutron in testing the flavor symmetry and final-state interaction was investigated. It was shown that the three-body nonleptonic decays are of great interest to explore the final-state interactions in $\Lambda_c^+$ decays.

Along this line, in the present work, we study the role of the $N^*(1535)$ resonance in the $\Lambda_c^+ \to \bar{K}^0\eta p$ decay by taking advantage of the strong coupling of the $N^*(1535)$ to the $\eta N$ channel and its large $uuds\bar{s}$ component. We calculate the invariant $\eta p$ mass distribution within the chiral unitary approach and an effective Lagrangian model. First, we follow the same approach used in Ref. [41] to study the $\Lambda_c^+ \to \pi^+ MB$ decays, but with the hadronization of the $uud$ rather than the $sud$ cluster to get the final $\eta p$ and from the $s\bar{d}$ pair to get the $\bar{K}^0$. In this respect, the $N^*(1535)$ resonance is dynamically generated from the final-state interaction of mesons and baryons in the $I = 1/2$ sector where we have assumed that the $ud$ diquark with $I = 0$ in the $\Lambda_c^+$ is a spectator. Second, we study the $\Lambda_c^+ \to \bar{K}^0 N^*(1535) \to \bar{K}^0\eta p$ decay at the hadron level by taking a Breit-Wigner formula to describe the distribution of the $N^*(1535)$ resonance within the effective Lagrangian model. The contributions from other low-lying $N^*$ and $\Sigma^*$ resonances are discussed. Fortunately, it is found that these contributions may not affect much the results obtained here.

This article is organized as follows. In Sec. II, we present the theoretical formalism of the decay of $\Lambda_c^+ \to \bar{K}^0\eta p$, explaining in detail the hadronization and final-state interactions of the $\eta p$ pair. Numerical results and discussions are presented in Sec. III, followed by a short summary in the last section.

## II. FORMALISM

As shown in Refs. [41,43,46], a Cabibbo allowed mechanism for the $\Lambda_c^+$ decay is that the charmed quark
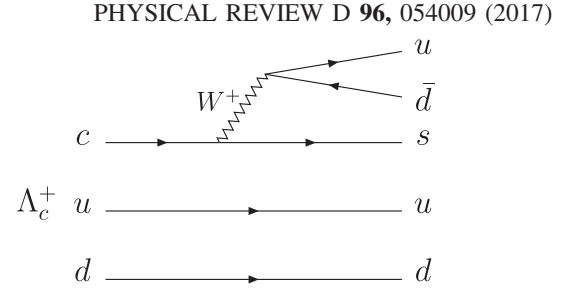


FIG. 1. Dominant diagram at the quark level for the charm quark in the $\Lambda_c^+$ decaying into a $u\bar{d}$ pair and a strange quark. The solid lines and the wiggly line stand for the quarks and the $W^+$ boson, respectively.

in $\Lambda_c^+$ turns into a strange quark with a $u\bar{d}$ pair by the weak interaction as shown in Fig. 1.

In addition to the $c$ quark decay process described above, in principle one can also have contributions from internal $W$-exchange $(c + d \to s + u)$ diagrams. As discussed in Refs. [41,43,46,47], these contributions are smaller than the $c$ decay process. Furthermore, including such contributions, the decay amplitudes would become more complex due to additional parameters from the weak interaction, and we cannot determine or constrain these parameters at present. Hence, we will leave these contributions to future studies when more experimental data become available.

### A. The $N^*(1535)$ as a dynamically generated state from meson-baryon scattering

We first discuss the decay of $\Lambda_c^+$ to produce the $\bar{K}^0$ from the $s\bar{d}$ pair and the insertion of a new $\bar{q}q$ pair with the quantum numbers of the vacuum, $\bar{u}u + \bar{d}d + \bar{s}s$, to construct the intermediate meson-baryon state $MB$ from the $uud$ cluster with the assumption that the $u$ and $d$ quarks in the $\Lambda_c^+$ are spectators in the weak decay corresponding to the mechanism of Fig. 2. Thus, after the hadronization these $u$ and $d$ quarks in the $\Lambda_c^+$ are part of the baryon, and the $u$ quark originated from the weak decay forms the meson. Furthermore, the $uud$ cluster with strangeness zero is combined into a pure $I = 1/2$ state:
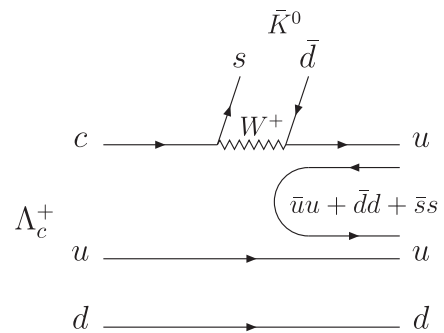


FIG. 2. Quark level diagram for the $\Lambda_c^+ \to \bar{K}^0 MB$ decay with the $\bar{K}^0$ emission from the $s\bar{d}$ pair.

$$\frac{1}{\sqrt{2}}|u(ud - du)\rangle. \qquad (1)$$

Following the procedure of Refs. [41,43,46,48,49], one can straightforwardly obtain the meson-baryon states after the $\bar{q}q$ pair production as

$$|MB\rangle = \frac{\sqrt{3}}{3}|\eta p\rangle + \frac{\sqrt{2}}{2}|\pi^0 p\rangle + |\pi^+ n\rangle - \frac{\sqrt{6}}{3}|K^+\Lambda\rangle, \qquad (2)$$

where we have omitted the $\eta' p$ term because of its large mass threshold compared to other channels that we considered.

After the production of a meson-baryon pair, the final-state interaction between them takes place, which can be parametrized by the rescattering shown in Fig. 3 at the hadronic level for the $\Lambda_c^+ \to \bar{K}^0 \eta p$ decay. The final-state interaction of $MB$, in $I = 1/2$, leads to the dynamical generation of the $N^*(1535)$ resonance [8,50]. In Fig. 3, we also show the tree level diagram for the $\Lambda_c^+ \to \bar{K}^0 \eta p$ decay.

According to Eq. (2), we can write down the $\Lambda_c^+ \to \bar{K}^0 \eta p$ decay amplitude of Fig. 3 as [51]

$$T^{MB} = V_P \left(\frac{\sqrt{3}}{3} + \frac{\sqrt{3}}{3} G_{\eta p}(M_{\eta p}) t_{\eta p \to \eta p}(M_{\eta p})\right.$$
$$+ \frac{\sqrt{2}}{2} G_{\pi^0 p}(M_{\eta p}) t_{\pi^0 p \to \eta p}(M_{\eta p})$$
$$+ G_{\pi^+ n}(M_{\eta p}) t_{\pi^+ n \to \eta p}(M_{\eta p})$$
$$\left. - \frac{\sqrt{6}}{3} G_{K^+\Lambda}(M_{\eta p}) t_{K^+\Lambda \to \eta p}(M_{\eta p})\right), \qquad (3)$$

where $V_P$ expresses the weak and hadronization strength, which is assumed to be a constant and independent of the final-state interaction. In the above equation, $G_{MB}$ denotes the one-meson-one-baryon loop function, which depends on the invariant mass of the final $\eta p$ system, $M_{\eta p}$. The meson-baryon scattering amplitudes $t_{MB \to \eta p}$ are those obtained in the chiral unitary approach, which depend also on $M_{\eta p}$. Details can be found in Refs. [8,50].

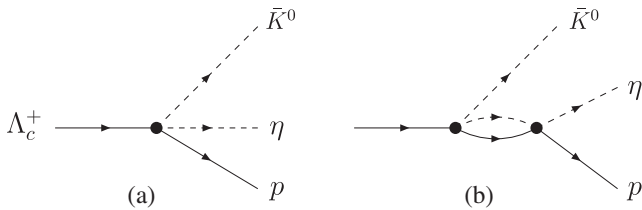FIG. 3. Diagrams for the $\Lambda_c^+ \to \bar{K}^0 \eta p$ decay: (a) direct $\bar{K}^0 \eta p$ vertex at tree level; (b) final-state interaction of the $\eta p$.
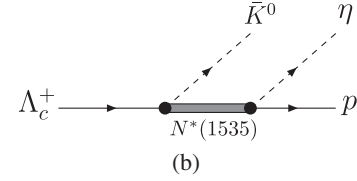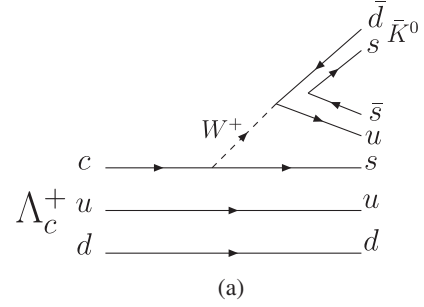
FIG. 4. (a) Quark level diagram for $\Lambda_c^+ \to \bar{K}^0 N^*(1535)$ and (b) hadron level diagram for $\Lambda_c^+ \to \bar{K}^0 \eta p$ decay.

## B. Effective Lagrangian approach and the $N^*(1535)$ resonance as a Breit-Wigner resonance

On the other hand, because the $N^*(1535)$ has a large $uuds\bar{s}$ component, it can also be produced via the process shown in Fig. 4(a), similar to the $P_c^+$ states produced in the $\Lambda_b^0 \to K^- P_c^+$ decay [52]. After the $N^*(1535)$ is formed with $uuds\bar{s}$, it decays into $\eta p$, which is the dominant decay channel of the $N^*(1535)$ resonance. We show the hadron level diagram for the decay of $\Lambda_c^+ \to \bar{K}^0 N^*(1535) \to \bar{K}^0 \eta p$ in Fig. 4(b).

Before going further, we emphasize that the strangeness component of $N^*(1535)$ cannot be guaranteed from the decay process shown in Fig. 4. Indeed, the $N^*(1535)$ can also be produced from the process shown in Fig. 2, where the $s\bar{d}$ forms the $\bar{K}^0$, while the $N^*(1535)$ is constructed from the $uud$ cluster and then it decays into $\eta p$ because of its large coupling to this channel.

The general decay amplitudes for $\Lambda_c^+ \to \bar{K}^0 N^*(1535)$ can be decomposed into two different structures with the corresponding coefficients $A$ and $B$,

$$\mathcal{M} = i\bar{u}(q)(A + B\gamma_5)u(p), \qquad (4)$$

where $q$ and $p$ are the momentum of the $N^*(1535)$ and $\Lambda_c^+$, respectively. The coefficients $A$ and $B$ for charmed baryons decaying into ground meson and baryon states, in general, can be calculated in the framework of the pole model [53] or within the perturbative QCD approach [54]. In the present case, because the $N^*(1535)$ resonance is not well understood in the classical quark model, the values of $A$ and $B$ in Eq. (4) are very difficult to pin down, and we have to determine them with future experimental data. In this work, we take $A = B$ and we come back to this issue later.

To get the whole decay amplitude of $\Lambda_c^+ \to \bar{K}^0 N^*(1535) \to \bar{K}^0 \eta p$ as shown in Fig. 4(b), we use the

effective Lagrangian density of Refs. [14,19,55] for the $N^*(1535)N\eta$ vertex,

$$\mathcal{L}_{N^*N\eta} = -ig_{N^*N\eta}\bar{N}\eta N^* + \text{H.c.}, \qquad (5)$$

where $N$, $\eta$, and $N^*$ represent the fields of the proton, the $\eta$ meson, and the $N^*(1535)$ resonance, respectively.

The invariant decay amplitude of the $\Lambda_c^+ \to \bar{K}^0 N^*(1535) \to \bar{K}^0 \eta p$ decay is

$$T^{N^*} = ig_{N^*N\eta}\bar{u}(p_3, s_p)G_{N^*}(q)(A + B\gamma_5)u(p, s_{\Lambda_c^+}), \qquad (6)$$

where $p_3$ is the momentum of the final proton. $s_p$ and $s_{\Lambda_c^+}$ are the spin polarization variables for the proton and $\Lambda_c^+$ baryon, respectively. $G_{N^*}(q)$ is the propagator of the $N^*(1535)$, which is given by a BW form as

$$G_{N^*}(q) = i\frac{\not{q} + M_{N^*}}{q^2 - M_{N^*}^2 + iM_{N^*}\Gamma_{N^*}(q^2)}, \qquad (7)$$

where $M_{N^*}$ and $\Gamma_{N^*}(q^2)$ are the mass and total decay width of the $N^*(1535)$, respectively. We take $M_{N^*} = 1535$ MeV as in the PDG [4]. For $\Gamma_{N^*}(q^2)$, since the dominant decay channels for the $N^*(1535)$ resonance are $\pi N$ and $\eta N$ [4], we take the following form as used in Refs. [56,57]:

$$\Gamma_{N^*}(q^2) = \Gamma_{N^* \to \pi N}(q^2) + \Gamma_{N^* \to \eta N}(q^2) + \Gamma_0, \qquad (8)$$

with

$$\Gamma_{N^* \to \pi N}(q^2) = \frac{3g_{N^*N\pi}^2}{4\pi}\frac{\sqrt{|\vec{p}_{N\pi}| + m_p^2} + m_p}{\sqrt{q^2}}|\vec{p}_{N\pi}|, \qquad (9)$$

$$\Gamma_{N^* \to \eta N}(q^2) = \frac{g_{N^*N\eta}^2}{4\pi}\frac{\sqrt{|\vec{p}_{N\eta}| + m_p^2} + m_p}{\sqrt{q^2}}|\vec{p}_{N\eta}|. \qquad (10)$$

Here

$$|\vec{p}_{N\pi}| = \frac{\lambda^{1/2}(q^2, m_p^2, m_\pi^2)}{2\sqrt{q^2}}, \qquad (11)$$

$$|\vec{p}_{N\eta}| = \frac{\lambda^{1/2}(q^2, m_p^2, m_\eta^2)}{2\sqrt{q^2}}, \qquad (12)$$

where $\lambda$ is the Källén function with $\lambda(x,y,z) = (x-y-z)^2 - 4yz$. In the present work, we take $g_{N^*N\pi}^2/4\pi = 0.037$ and $g_{N^*N\eta}^2/4\pi = 0.28$ as used in Ref. [58]. With these values we can get $\Gamma_{N^* \to N\pi} = 67.5$ MeV and $\Gamma_{N^* \to N\eta} = 63$ MeV if we take $\sqrt{q^2} = 1535$ MeV. In this work, we choose $\Gamma_0 = 19.5$ MeV for $\Gamma_{N^*}(\sqrt{q^2} = 1535$ MeV$) = 150$ MeV.

In the effective Lagrangian approach, the sum over polarizations and the Dirac spinors can be easily done thanks to

$$\sum_{s_p}\bar{u}(p_3, s_p)u(p_3, s_p) = \frac{\not{p}_3 + m_p}{2m_p}, \qquad (13)$$

$$\sum_{s_{\Lambda_c^+}}\bar{u}(p, s_{\Lambda_c^+})u(p, s_{\Lambda_c^+}) = \frac{\not{p} + M_{\Lambda_c^+}}{2M_{\Lambda_c^+}}. \qquad (14)$$

Finally, we obtain

$$\frac{1}{2}\overline{\sum_{s_{\Lambda_c^+}}}\sum_{s_p}|T^{N^*}|^2 = \frac{g_{N^*N\eta}^2}{2m_pM_{\Lambda_c^+}|D|^2}$$
$$\times [(ap \cdot q + bp_3 \cdot p + cM_{\Lambda_c^+})A^2 + (ap \cdot q + bp_3 \cdot p - cM_{\Lambda_c^+})B^2], \qquad (15)$$

with

$$D = q^2 - M_{N^*}^2 + iM_{N^*}\Gamma_{N^*}(q^2), \qquad (16)$$

$$a = 2(p_3 \cdot q + m_pM_{N^*}), \qquad (17)$$

$$b = M_{N^*}^2 - q^2, \qquad (18)$$

$$c = m_p(M_{N^*}^2 + q^2) + 2M_{N^*}p_3 \cdot q, \qquad (19)$$

and

$$p \cdot q = \frac{M_{\Lambda_c^+}^2 + M_{\eta p}^2 - m_{\bar{K}^0}^2}{2}, \qquad (20)$$

$$p_3 \cdot q = \frac{M_{\eta p}^2 + m_p^2 - m_\eta^2}{2}, \qquad (21)$$

$$p_3 \cdot p = \frac{(M_{\Lambda_c^+}^2 + M_{\eta p}^2 - m_{\bar{K}^0}^2)(M_{\eta p}^2 + m_p^2 - m_\eta^2)}{2M_{\eta p}^2}, \qquad (22)$$

with $M_{\eta p}^2 = q^2$.

### C. Invariant mass distributions of the $\Lambda_c^+ \to \bar{K}^0\eta p$ decay

With all the ingredients obtained in the previous subsection, one can write down the invariant $\eta p$ mass distribution of the $\Lambda_c^+ \to \bar{K}^0\eta p$ decay as

$$\frac{d\Gamma}{dM_{\eta p}} = \frac{1}{16\pi^3}\frac{m_p p_{\bar{K}^0} p_\eta^*}{M_{\Lambda_c^+}}|T|^2, \qquad (23)$$

where $T$ is the total decay amplitude. The $p_{\bar{K}^0}$ and $p_\eta^*$ are the three-momenta of the outgoing $\bar{K}^0$ meson in the $\Lambda_c^+$ rest

frame and the outgoing $\eta$ meson in the center of mass frame of the final $\eta p$ system, respectively. They are given by

$$p_{\bar{K}^0} = \frac{\lambda^{1/2}(M^2_{\Lambda^+_c}, M^2_{\eta p}, m^2_{\bar{K}^0})}{2M_{\Lambda^+_c}}, \qquad (24)$$

$$p^*_\eta = \frac{\lambda^{1/2}(M^2_{\eta p}, m^2_\eta, m^2_p)}{2M_{\eta p}}. \qquad (25)$$

The range of $M_{\eta p}$ is

$$M^{\max}_{\eta p} = M_{\Lambda^+_c} - m_{\bar{K}^0},$$
$$M^{\min}_{\eta p} = m_\eta + m_p.$$

## III. NUMERICAL RESULTS AND DISCUSSION

In this section, we first show the numerical results for the $d\Gamma/dM_{\eta p}$ with four models: Model I takes $T = T^{MB}$; Model II takes $T = T^{N^*}$, $M_{N^*} = 1535$ MeV, and $\Gamma_{N^*}$ is energy dependent as in Eq. (8); Model III takes $T = T^{N^*}$, $M_{N^*} = 1543$ MeV, and $\Gamma_{N^*} = 92$ MeV as the pole parameters obtained in Ref. [8], where the $N^*(1535)$ is a dynamically generated state; Model IV takes $T = T^{N^*}$, $M_{N^*} = 1500$ MeV, and $\Gamma_{N^*} = 110$ MeV as the averaged pole parameters obtained in Refs. [33–37] from partial wave analysis of the pion- and photon-induced reactions. Next, we will discuss the impact of the contributions from other $N^*$ and $\Sigma^*$ states.

### A. Invariant $\eta p$ mass distributions

In Fig. 5, we show the $\eta p$ invariant mass distribution obtained with the mass values shown in Table I, where the solid, dashed, dotted, and dashed-dotted curves represent the numerical results obtained with Model I, II, III, and IV,
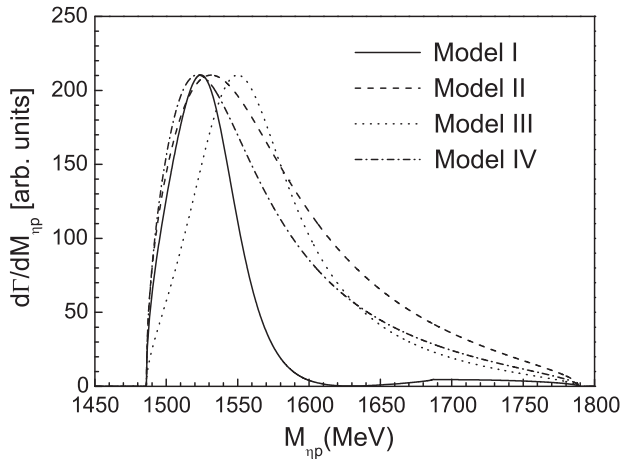


FIG. 5. Invariant $\eta p$ mass distribution for the $\Lambda^+_c \to \bar{K}^0 \eta p$ decay. The solid, dashed, dotted, and dashed-dotted curves represent the results obtained in Model I, II, III, and IV, respectively.

TABLE I. Masses and spin-parities of the particles studied in the present work.

| State | Mass (MeV) | Spin-parity ($J^P$) |
|---|---|---|
| $\Lambda^+_c$ | 2286.46 | $\frac{1}{2}^+$ |
| $\bar{K}^0$ | 497.61 | $0^-$ |
| $\eta$ | 547.86 | $0^-$ |
| $p$ | 938.27 | $\frac{1}{2}^+$ |

respectively. The results of Model I are obtained with $V_P = 1$ MeV$^{-1}$. The results of Model II with $A = B = 47.2$, Model III with $A = B = 27.7$, and Model IV with $A = B = 39.5$ are normalized to the peak of Model I.

For Model I, a peak around 1524 MeV corresponding to the $N^*(1535)$ resonance can be clearly seen as in Ref. [50], which is lower by 26 MeV than the peak of Model III. The peaks of Models II and IV move to 1532 and 1522 MeV, respectively. The peak position of Model II is very close to the central value, 1535 MeV, estimated in the PDG [4] for the $N^*(1535)$. The peak position of Model I is also close to the value 1535 MeV, but with a narrow width. For Model IV, where the pole parameters of the $N^*(1535)$ obtained from the partial wave analysis are used, the peak position is very similar to the one of Model I. However, the resonant shapes of Models II, III, and IV are broader than the result of Model I.

Because the mass of the $N^*(1535)$ is close to the $\eta N$ threshold and has a large coupling to this channel, the approximation of a BW form with a constant width is not very realistic [14]. We should take the coupled-channel BW formula as in Eq. (8), which will reduce the BW mass of the $N^*(1535)$ [14].

From the results of Models I and II shown in Fig. 5, we see that these two different descriptions of the $N^*(1535)$ resonance give different invariant $\eta p$ mass distributions. The findings here are similar to those obtained in Refs. [15,20]. For the $N^*(1535)$, the amplitude square obtained with the chiral unitary approach does not behave like a usual BW resonance, even at the peak position (see Fig. 1 of Ref. [15]). Note that in the chiral unitary approach, only the meson-baryon components of $N^*(1535)$ are included. However, in the works of Refs. [59,60], it was shown that the $N^*(1535)$ contains a mixture of a genuine quark state apart from the meson-baryon components.[1] We

---

[1]After an amplitude for the nonresonant contributions is included, the pole position of the $N^*(1535)$ is obtained as [59]

$$\sqrt{s_R} = 1537 - i37 (\text{MeV}) \qquad (26)$$

for the $n^*$ (neutron charge) and

$$\sqrt{s_R} = 1532 - i37 (\text{MeV}) \qquad (27)$$

for the $p^*$ (+1 charge).

expect that future experimental measurements may test our model predictions and clarify this issue.

One might be tempted to think that the discrepancy between Models I and II is due to the inclusion of the $p$-wave contribution for Model II shown in Eq. (4) with the $B$ term. We have explored such a possibility from the comparison of the contributions of the $A$ and $B$ terms. For doing this, we first rewrite $d\Gamma/dM_{\eta p}$ for Model II as

$$\frac{d\Gamma}{dM_{\eta p}} = f_1 A^2 + f_2 B^2. \tag{28}$$

Then we define the ratio $R$ as

$$R = \frac{f_2 B^2}{f_1 A^2} = \frac{f_2}{f_1}. \tag{29}$$

In the last step, we have taken $A = B$.

In Fig. 6 we show the numerical results for $R$ as a function of $M_{\eta p}$. We see clearly that $R$ is less than 2.8% for the whole possible $M_{\eta p}$ in the $\Lambda_c^+ \to \bar{K}^0 \eta p$ decay. This means that the contribution of the $p$-wave $B$ term is rather small in comparison with the contribution from the $s$-wave $A$ term and can be neglected safely. This study provides further support for the factorization scheme of the hard process (the weak decay and hadronization) for Model I, where only the $s$-wave contribution is considered between any two particles of the final $\bar{K}^0 \eta p$. Such a factorization scheme seems to work fairly well in the present case.

It should be noted that the $B$ term is very small compared with the $A$ term, which is tied to the fact that we take $A = B$. A model independent calculation of the values of $A$ and $B$ is most welcome and will ultimately test our model calculations.
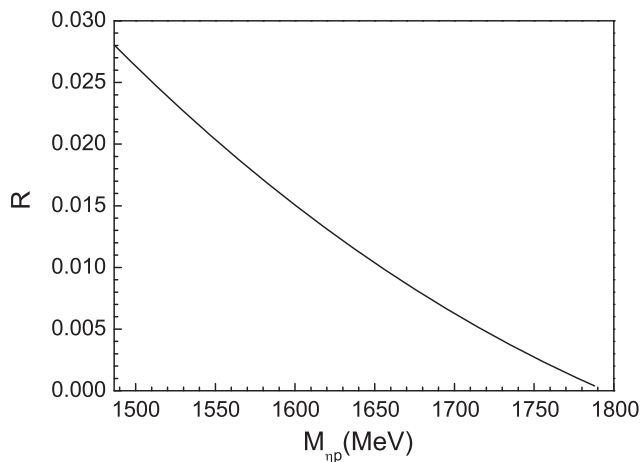


FIG. 6. Ratio $R$ of the $B$ and $A$ terms as a function of the $\eta p$ invariant mass.

## B. Contributions from other processes

Up to now, we have considered only the contribution from $N^*(1535)$, while the contributions from other nucleon resonances, such as $N^*(1650)\frac{1}{2}^-$, $N^*(1710)\frac{1}{2}^+$, and $N^*(1720)\frac{3}{2}^+$, are not taken into account. The $N^*(1710)$ and $N^*(1720)$ decay into $\eta p$ in $p$-waves and the decay of $\Lambda_c^+ \to \bar{K}^0 N^*(1710)$ and $\Lambda_c^+ \to \bar{K}^0 N^*(1720)$ have very limited phase space; hence, their contributions should be much suppressed.

It is interesting to note that both the $N^*(1535)$ and the $N^*(1650)$ are dynamically generated from the analysis of the $s$-wave $\pi N$ scattering [7,9]. We list the results obtained in Refs. [7,9–13] for the $N^*(1535)$ and the $N^*(1650)$ in Table II, where we have taken the pole position as $\sqrt{s_R} = M_R - i\Gamma_R/2$. We see that the $N^*(1650)$ and the $N^*(1535)$ are greatly separated in mass.

Yet, it is well known that the interference between the $N^*(1535)$ and the $N^*(1650)$ is crucial to describe the $\pi N \to \eta N$ and $\gamma N \to \eta N$ scattering data [62–64]. In particular, the narrow structure observed in the total cross section and the behavior of the angular distributions of the $\gamma n \to \eta n$ experimental data [65–67] can be understood quantitatively as interference between the $N^*(1535)$ and the $N^*(1650)$ [36,64]. In fact, the branching ratio of the $N^*(1650)$ to $\eta N$, Br$[N^*(1650) \to \eta N] = (18 \pm 4)\%$, is sizable compared with the one to $\pi N$, Br$[N^*(1650) \to \pi N] = (60 \pm 10)\%$ [4]. The very recent analysis of the $\gamma p \to \eta p$ in Ref. [68] gives Br$[N^*(1650) \to \eta N] = (28 \pm 11)\%$. In addition, the value of Br$[N^*(1650) \to \eta N] = (32 \pm 4)\%$ was reported in Ref. [69] from the latest analysis by including the polarization data. On the other hand, from the coupled-channel analysis of $\eta$ meson production including all recent photoproduction data on the proton, the value of $1 \pm 2\%$ is obtained in Ref. [36] and of 1.4% in Ref. [70]. However, the branching ratios of Refs. [36,70] were obtained from the fitted couplings with the $K$-matrix formula at the resonance mass. Since the total width of the $N^*(1650)$ is energy dependent and the $N^*(1650)N\eta$ vertex is modified by form factors, the branching ratios obtained in Refs. [36,70] are model dependent [71].

TABLE II. Mass ($M_R$) and width ($\Gamma_R$) for $N^*(1535)$ and $N^*(1650)$ found in Refs. [7,9–13]. The values of masses and widths are given in MeV.

| | $N^*(1535)$ | | $N^*(1650)$ | |
|---|---|---|---|---|
| Reference | $M_R$ | $\Gamma_R$ | $M_R$ | $\Gamma_R$ |
| [7] | 1496.5 ± 0.4 | 83.3 ± 0.7 | 1684.3 ± 0.7 | 194.3 ± 0.8 |
| [9] | 1506 | 280 | 1692 | 92 |
| [10,11] | 1556 | 94 | 1639 | 76 |
| [12] | 1504 | 110 | 1668 | 56 |
| | | | 1673 | 134[a] |
| [13] | 1508.1 | 90.3 | 1672.3 | 158.2 |

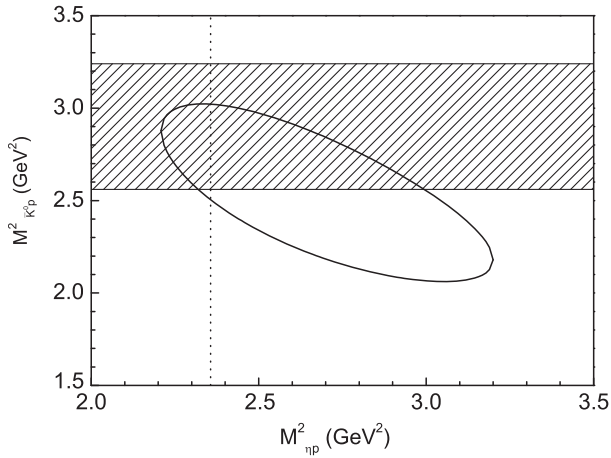[a] A twin pole structure for $N^*(1650)$ was obtained in Ref. [61].

FIG. 7. Dalitz plot for $M^2_{\eta p}$ and $M^2_{\bar{K}^0 p}$ in the $\Lambda_c^+ \to \bar{K}^0 \eta p$ decay. The $N^*(1535)$ energy is shown by the vertical dotted line, and the horizontal band represents the masses of $\Sigma^*$ states from 1600 to 1800 MeV.

Nevertheless, the production mechanism of the $N^*(1650)$ in the $\Lambda_c^+ \to \bar{K}^0 \eta p$ decay might be different from those in the pion- and photon-induced reactions. Furthermore, considering the contribution from the $N^*(1650)$ at this stage introduces unavoidably more parameters with no experimental constraints. We will leave a detailed study of the possible interference from the $N^*(1650)$ to future works and hope that future experimental data are good enough to disentangle the contributions of these two resonances to the $\Lambda_c^+ \to \bar{K}^0 \eta p$ decay so that we can learn more about the $N^*(1535)$.

On the other hand, there should also be contributions from $\Sigma^*$ resonances that have a significant branching ratio to $\bar{K}^0 p$. Those $\Sigma^*$ resonances are $\Sigma^*(1660)\frac{1}{2}^+$, $\Sigma^*(1670)\frac{3}{2}^-$, and $\Sigma^*(1750)\frac{1}{2}^-$. We show the Dalitz plot for the $\Lambda_c^+ \to \bar{K}^0 \eta p$ decay in Fig. 7. In the $N^*(1535)$ energy region, the Dalitz plot overlaps with these $\Sigma^*$ resonances from 1600 to 1800 MeV in the $\bar{K}^0 p$ channel, which may make the analysis of $N^*(1535)$ difficult. Fortunately, the $\Sigma^*(1660)\frac{1}{2}^+$ and $\Sigma^*(1670)\frac{3}{2}^-$ decay into $\bar{K}^0 p$ in $p$-waves and $D$-waves, respectively. These contributions will be suppressed because of the higher partial waves involved. For the $\Sigma^*(1750)\frac{1}{2}^-$, it decays into $\bar{K}^0 p$ in $s$-waves. However, it lies in the kinematic end-point region and therefore the decay of $\Lambda_c^+ \to \eta \Sigma^*(1750)$ has a relatively small phase space.

In summary, the contributions from other $N^*$ and $\Sigma^*$ resonances are expected to be small compared with the contribution from the $N^*(1535)$ [perhaps except the $N^*(1650)$ that is less clear] and not to change much the model predictions here. If future experimental measurements provide enough data to disentangle the contributions

from these resonances, one can also study them. It should be kept in mind that our study made some assumptions and hence it can be improved once more data become available.

## IV. CONCLUSIONS

In the present work we have studied the invariant $\eta p$ mass distribution in the $\Lambda_c^+ \to \bar{K}^0 \eta p$ decay to better understand the $N^*(1535)$ resonance. First, we employed the molecular picture where the $N^*(1535)$ is dynamically generated from the meson-baryon interaction. In such a scenario, the weak interaction part is dominated by the $c$ quark decay process, $c(ud) \to (s + u + \bar{d})(ud)$, while the hadronization part takes place by the $uud$ cluster picking up a $q\bar{q}$ pair from the vacuum and hadronizes into a meson-baryon pair, and the $s\bar{d}$ pair from the weak decay turns into a $\bar{K}^0$. The following final-state interactions of the meson-baryon pairs are described in the chiral unitary model that dynamically generates the $N^*(1535)$ resonance in the $I = 1/2$ sector. Second, we studied the $\Lambda_c^+ \to \bar{K}^0 N^*(1535) \to \bar{K}^0 \eta p$ decay with a Breit-Wigner formula to describe the distribution of the $N^*(1535)$ in the effective Lagrangian model. The above two descriptions for the $N^*(1535)$ resonance give different invariant $\eta p$ mass distributions. Furthermore, we showed in a qualitative way that the contributions from other $N^*$ and $\Sigma^*$ resonances are relatively small and will not affect much the results obtained in the present study.

On the experimental side, the decay mode $\Lambda_c^+ \to \bar{K}^0 \eta p$ has been observed [4,72] and the branching ratio Br($\Lambda_c^+ \to \bar{K}^0 \eta p$) is determined to be $(1.6 \pm 0.4)\%$, which is one of the dominant decay modes of the $\Lambda_c^+$ state. For the decay of $\Lambda_c^+ \to \bar{K}^0 \eta p$, the final $\eta p$ is in pure isospin $I = 1/2$. Hence, this decay can be an ideal process to study the $N^*(1535)$ resonance, which has a large branching ratio to $\eta N$ and decays into $\eta N$ in $s$-waves. Future experimental measurements of the invariant $\eta p$ mass distribution studied in the present work will be very helpful to test our model calculations and constrain the properties of the $N^*(1535)$ resonance. For example, a corresponding experimental measurement could in principle be done at BESIII [73] and Belle.

[1] E. Klempt and A. Zaitsev, Phys. Rep. **454**, 1 (2007).
[2] V. Crede and W. Roberts, Rep. Prog. Phys. **76**, 076301 (2013).
[3] S. Capstick and W. Roberts, Prog. Part. Nucl. Phys. **45**, S241 (2000).
[4] C. Patrignani *et al.* (Particle Data Group), Chin. Phys. C **40**, 100001 (2016).
[5] N. Kaiser, P. B. Siegel, and W. Weise, Phys. Lett. B **362**, 23 (1995).
[6] N. Kaiser, T. Waas, and W. Weise, Nucl. Phys. **A612**, 297 (1997).
[7] J. Nieves and E. Ruiz Arriola, Phys. Rev. D **64**, 116008 (2001).
[8] T. Inoue, E. Oset, and M. J. Vicente Vacas, Phys. Rev. C **65**, 035204 (2002).
[9] P. C. Bruns, M. Mai, and U. G. Meissner, Phys. Lett. B **697**, 254 (2011).
[10] J. Nieves, A. Pich, and E. Ruiz Arriola, Phys. Rev. D **84**, 096002 (2011).
[11] D. Gamermann, C. Garcia-Recio, J. Nieves, and L. L. Salcedo, Phys. Rev. D **84**, 056017 (2011).
[12] K. P. Khemchandani, A. Martinez Torres, H. Nagahiro, and A. Hosaka, Phys. Rev. D **88**, 114016 (2013).
[13] E. J. Garzon and E. Oset, Phys. Rev. C **91**, 025201 (2015).
[14] B. C. Liu and B. S. Zou, Phys. Rev. Lett. **96**, 042002 (2006).
[15] L. S. Geng, E. Oset, B. S. Zou, and M. Döring, Phys. Rev. C **79**, 025203 (2009).
[16] T. Mart, Phys. Rev. C **87**, 042201 (2013).
[17] M. Dugger *et al.* (CLAS Collaboration), Phys. Rev. Lett. **96**, 062001 (2006); **96**, 169905(E) (2006).
[18] X. Cao and X. G. Lee, Phys. Rev. C **78**, 035207 (2008).
[19] J. J. Xie, B. S. Zou, and H. C. Chiang, Phys. Rev. C **77**, 015206 (2008).
[20] M. Döring, E. Oset, and B. S. Zou, Phys. Rev. C **78**, 025207 (2008).
[21] X. Cao, J. J. Xie, B. S. Zou, and H. S. Xu, Phys. Rev. C **80**, 025203 (2009).
[22] C. Helminen and D. O. Riska, Nucl. Phys. **A699**, 624 (2002).
[23] B. S. Zou, Eur. Phys. J. A **35**, 325 (2008).
[24] C. S. An and B. S. Zou, Eur. Phys. J. A **39**, 195 (2009).
[25] C. S. An, Chin. Phys. C **33**, 1393 (2009).
[26] B. S. Zou, Nucl. Phys. **A835**, 199 (2010).
[27] R. A. Arndt, W. J. Briscoe, I. I. Strakovsky, and R. L. Workman, Phys. Rev. C **74**, 045205 (2006).
[28] M. Doring, C. Hanhart, F. Huang, S. Krewald, and U.-G. Meissner, Nucl. Phys. **A829**, 170 (2009).
[29] A. V. Anisovich, E. Klempt, V. A. Nikonov, M. A. Matveev, A. V. Sarantsev, and U. Thoma, Eur. Phys. J. A **44**, 203 (2010).
[30] M. Doring and K. Nakayama, Eur. Phys. J. A **43**, 83 (2010).
[31] M. Batinic, S. Ceci, A. Svarc, and B. Zauner, Phys. Rev. C **82**, 038203 (2010).
[32] R. L. Workman, M. W. Paris, W. J. Briscoe, and I. I. Strakovsky, Phys. Rev. C **86**, 015202 (2012).
[33] M. Shrestha and D. M. Manley, Phys. Rev. C **86**, 055203 (2012).
[34] A. V. Anisovich, R. Beck, E. Klempt, V. A. Nikonov, A. V. Sarantsev, and U. Thoma, Eur. Phys. J. A **48**, 15 (2012).
[35] D. Ronchen, M. Döring, F. Huang, H. Haberzettl, J. Haidenbauer, C. Hanhart, S. Krewald, U. -G. Meißner, and K. Nakayama, Eur. Phys. J. A **49**, 44 (2013).
[36] V. Shklyar, H. Lenske, and U. Mosel, Phys. Rev. C **87**, 015201 (2013).
[37] H. Kamano, S. X. Nakamura, T.-S. H. Lee, and T. Sato, Phys. Rev. C **88**, 035209 (2013).
[38] D. Ronchen, M. Doring, H. Haberzettl, J. Haidenbauer, U.-G. Meißner, and K. Nakayama, Eur. Phys. J. A **51**, 70 (2015).
[39] V. Crede and C. A. Meyer, Prog. Part. Nucl. Phys. **63**, 74 (2009).
[40] H. X. Chen, W. Chen, X. Liu, and S. L. Zhu, Phys. Rep. **639**, 1 (2016).
[41] K. Miyahara, T. Hyodo, and E. Oset, Phys. Rev. C **92**, 055204 (2015).
[42] T. Hyodo and M. Oka, Phys. Rev. C **84**, 035201 (2011).
[43] J. J. Xie and L. S. Geng, Eur. Phys. J. C **76**, 496 (2016).
[44] J. J. Xie and L. S. Geng, Phys. Rev. D **95**, 074024 (2017).
[45] C. D. Lü, W. Wang, and F. S. Yu, Phys. Rev. D **93**, 056008 (2016).
[46] K. Miyahara, T. Hyodo, M. Oka, J. Nieves, and E. Oset, Phys. Rev. C **95**, 035212 (2017).
[47] J. J. Xie, L. R. Dai, and E. Oset, Phys. Lett. B **742**, 363 (2015).
[48] L. Roca, M. Mai, E. Oset, and U. G. Meißner, Eur. Phys. J. C **75**, 218 (2015).
[49] A. Feijoo, V. K. Magas, A. Ramos, and E. Oset, Phys. Rev. D **92**, 076015 (2015).
[50] M. Doring, E. Oset, and D. Strottman, Phys. Rev. C **73**, 045209 (2006).
[51] J. A. Oller and E. Oset, Nucl. Phys. **A629**, 739 (1998).
[52] R. Aaij *et al.* (LHCb Collaboration), Phys. Rev. Lett. **115**, 072001 (2015).
[53] H. Y. Cheng and B. Tseng, Phys. Rev. D **46**, 1042 (1992); **55**, 1697(E) (1997).
[54] C. D. Lü, Y. M. Wang, H. Zou, A. Ali, and G. Kramer, Phys. Rev. D **80**, 034011 (2009).
[55] J. Z. Bai *et al.* (BES Collaboration), Phys. Lett. B **510**, 75 (2001).
[56] J. J. Wu, S. Dulat, and B. S. Zou, Phys. Rev. C **81**, 045210 (2010).
[57] J. J. Xie, B. C. Liu, and C. S. An, Phys. Rev. C **88**, 015203 (2013).
[58] Q. F. Lü, R. Wang, J. J. Xie, X. R. Chen, and D. M. Li, Phys. Rev. C **91**, 035204 (2015).
[59] D. Jido, M. Doering, and E. Oset, Phys. Rev. C **77**, 065207 (2008).
[60] T. Hyodo, D. Jido, and A. Hosaka, Phys. Rev. C **78**, 025203 (2008).
[61] R. A. Arndt, I. I. Strakovsky, R. L. Workman, and M. M. Pavan, Phys. Rev. C **52**, 2120 (1995).
[62] X. H. Zhong, Q. Zhao, J. He, and B. Saghai, Phys. Rev. C **76**, 065205 (2007).
[63] M. Doring and K. Nakayama, Phys. Lett. B **683**, 145 (2010).
[64] A. V. Anisovich, E. Klempt, B. Krusche, V. A. Nikonov, A. V. Sarantsev, U. Thoma, and D. Werthmller, Eur. Phys. J. A **51**, 72 (2015).

[65] A. V. Anisovich, I. Jaegle, E. Klempt, B. Krusche, V. A. Nikonov, A. V. Sarantsev, and U. Thoma, Eur. Phys. J. A **41**, 13 (2009).

[66] D. Werthmüller *et al.* (A2 Collaboration), Phys. Rev. Lett. **111**, 232001 (2013).

[67] D. Werthmüller *et al.* (A2 Collaboration), Phys. Rev. C **90**, 015205 (2014).

[68] V. L. Kashevarov *et al.* (A2 Collaboration), Phys. Rev. Lett. **118**, 212001 (2017).

[69] U. Thoma, in International Workshop on Partial Wave Analyses and Advanced Tools for Hadron Spectroscopy (PWA9/ATHOS4), March 13–17, 2017, Bonn, Germany (unpublished), https://indico.cern.ch/event/591374/contributions/2486735.

[70] V. Shklyar, H. Lenske, U. Mosel, and G. Penner, Phys. Rev. C **71**, 055206 (2005); **72**, 019903(E) (2005).

[71] T. P. Vrana, S. A. Dytman, and T. S. H. Lee, Phys. Rep. **328**, 181 (2000).

[72] R. Ammar *et al.* (CLEO Collaboration), Phys. Rev. Lett. **74**, 3534 (1995).

[73] M. Ablikim *et al.* (BESIII Collaboration), Phys. Rev. Lett. **116**, 052001 (2016).